DOI: 10.21062/mft.2024.026 http://www.journalmt.com

The Manufacturing of Environmental Barrier Coatings by HV-APS Plasma Spraying Using Er_2O_3 and SiO_2 Powder Mixture

Paweł Pędrak (0000-0001-5862-6792), Tadeusz Kubaszek (0000-0002-7006-4857), Barbara Kościelniak (0000-0002-1683-0354), Marek Góral (0000-0002-7058-510X), Mateusz Micał
Research and Development Laboratory for Aerospace Materials, Rzeszow University of Technology, Powstancow Warszawy 12, 35-959 Rzeszow, Poland. Corresponding author's e-mail: mgoral@prz.edu.pl

Over the last decades, nickel-based superalloys with TBC coatings have been used as the main material for hot section turbine parts. The next step in the development of engines and increasing the combustion temperature is the use of Ceramic Matrix Composites (CMC). Nevertheless, in the presence of water vapour or molten salts, accelerated degradation of substrate material. These problems can be prevented by additional layers or coatings produced on its surface, or combinations of layers and coatings that form Environmental Barrier Coatings (EBCs). The aim of the research was the preparation of samples of a mixture of erbium oxide powders with silicon oxide with the addition of: polyvinyl alcohol, starch and cellulose gum. Then their technological properties were examined. A mixture with the most favourable properties was selected and sprayed using HV-APS method using with various process parameters and investigated. Conducted research showed that energy of HV-APS process is too low for synthesis of erbium disilicate in the resulting coating. The material was only melted, not vaporized. Making powder agglomerates with an average size of 150 μm with the addition of 3% PVA leads to a significant decrease in the surface area of powder grains. This results in a significant increase in flowability and allows it to be used as a charge material for APS plasma spraying.

Keywords: Plasma spray, Environmental barrier coatings, EBC, TBC, HV-APS, Er_2O_3, SiO_2

1 Introduction

Gas turbine engines are the backbone of the fast-growing aerospace and energy sectors [1-3]. Over the last decades, nickel-based superalloys with TBC coatings have been used as the main material for components and subassemblies of hot turbine parts, which can operate at gas combustion temperatures up to 1500°C [4-7]. Nevertheless, this strategy is approaching the limit imposed by melting point of the base material. The next step in the development of engines and increasing the combustion temperature is the use of Ceramic Matrix Composites (CMC), based on silicon carbide (SiC), which are the most promising material to fulfill this role [8]. Compared to nickel-based superalloys, CMCs provide higher operating temperatures and have better mechanical properties at elevated temperatures [9]. In a clean, dry oxygen atmosphere, SiC-based CMCs exhibit very good oxidation resistance due to the formation of a protective layer of silicon oxide [10]. Nevertheless, in the presence of water vapour [11] or molten salts [12], accelerated degradation of the protective layer of silicon oxide occurs, which results in accelerated degradation of the substrate material.

CMC corrosion problems can be prevented by additional layers or coatings produced on its surface, or combinations of layers and coatings that form Environmental Barrier Coatings (EBCs) [13,14]. The development of EBC coatings has changed the structure of coatings from single layer to multilayer [15]. Three-layer coatings are most often used usually composed of a bonding layer of pure silicon, an intermediate layer of mullite and a top layer [16]. Since Si and mullite are the preferred bonding coating and intermediate layer for SiC-based composites, materials for the top layer are sought [17]. The most promising group of materials for the surface layer are rare-earth silicates [18]. The surface layer of rare-earth metal silicates is characterized by a high melting point [19], good resistance to water vapor [20] and CMAS corrosion [21].

In our previous research we investigated potential materials for TBC/EBC using developed Reactive PS-PVD process (Plasma Spray Physical Vapour Deposition) [22]. The using of conventional Ytterbium Monosilicate deposited by Atmospheric Plasma Spraying as well as PS-PVD process was also investigated [23]. The aim of the work was to prepare a powder material by selecting the proportion of the content of erbium oxide and silicon oxide and organic additives that improve its technological properties, in particular flowability [24]. The mixture with the best properties was used in the APS atmospheric pressure plasma spraying process to determine the possibility

of synthesis of the erbium disilicate layer in the plasma plume similarly to observe in Reactive PS-PVD process [25]. The scope of work included the preparation of samples of a mixture of erbium oxide powders with silicon oxide with the addition of: polyvinyl alcohol, starch and cellulose gum. Then their technological properties were examined. A mixture with the most favourable properties was selected and sprayed using HV-APS method using with various process parameters [26]. In the next stage, observations of the microstructure, analysis of the chemical composition on the cross-section of the layer and the phase analysis using the XRD method were carried out.

2 Experimental

2.1 Preparation of mixtures of silicon and erbium oxide powders

Silicon oxide (SiO_2) with a purity of 99.6% erbium oxide (Er2O3) with a purity of 99.9% (Avantor Performance Materials) was used to prepare the mixtures of erbium and silicon oxide powders. The mixture of powders of both oxides was prepared in batches in the proportion of silicon oxide: erbium oxide 2:1 (76.9 wt. %: 23.05 wt. %). A part of the prepared mixture was used to make a standard sample - a tablet: the mixture was compressed on a mechanical press under a pressure of 298.4 N/cm^2. The prepared tablet was heated at 1500°C for 20 hours. Then, various organic binders were added to the prepared mixture and granules were produced (Tab. 1).

The production of granulates consisted in preliminary mixing and grinding in a planetary mill of appropriate amounts of oxide powders. The next step was to prepare a plastic mass by adding an aqueous binder solution to the mixture of powders, and then making granules by pressing through a sieve (mesh no. 22). The obtained granulate was dried for 24 h at 60°C. After drying, the obtained granulate was further sieved through the same sieve to remove large agglomerates formed during drying.

Tab. 1 *Content wt. % addition of a binder to the mixture of oxides*

Component	wt.%	
PVA	3.0	5.0
Pregelatinized starch	3.0	5.0
Cellulose gum (as CMC-Na sodium salt)	3.0	5.0

2.2 Characterization of the obtained granulates

The technological properties were characterized and the particle size of pure oxides and the produced granules was determined. Characteristics of technological properties were made using the PowderPro device. The main parameter for powders and granulates was the flow coefficient. The flow coefficient Fc is the sum of the values corresponding to the values of the coefficients obtained in the tests and calculated in accordance with the formula (1).

$$Fc = Aif + C + Afs + h \quad [a.u.] \qquad (1)$$

Where:

Aif…Index value corresponding to the value of the angle of internal friction,

C…Index value corresponding to the percentage of compressibility,

Afs…Index value corresponding to the value of the angle of the flat surface,

h…The index value corresponding to the homogeneity value.

The value of the flow coefficient (Fc) , i.e. the closer it is to 100 [a.u.], the better the given powder is transported in pneumatic systems and does not require the use of additional devices supporting to transport.

Observations of the morphology of the produced powders were conducted using a scanning electron microscope (SEM) Phenom XL with the use of a backscattered electron detector (BSE). The chemical composition of individual powder components was analysed using an X-ray energy dispersion spectrometer (EDS). Chemical composition tests were performed in micro-areas at an accelerating voltage of 15 kV, obtaining maps of the relative content of elements from the studied areas.

Powder grain sizes - determined using a KμK device, model IPS U, by diffraction of infrared laser light. The distribution of the average grain diameter in the range from 0.5 to 1000 μm was determined.

2.3 Production of EBCs using the plasma spraying method

Ceramic layers were made on a substrate of Inconel 625 alloy with a metallic bond coat produced in by conventional atmospheric plasma spraying (APS) method using Amdry 386 (Oerlikon-Metco, Switzerland) powder containing (wt.%): Co–23%; Cr-17%; Al-12%; Y–0.45%; Ni-prom. The detailed process parameters were based on our previous research [27] using parameters (Tab. 2), The ceramic layers were produced by HV-APS (High Velocity- Atmospheric Plasma Spraying) method using the Thermico system with an Axial III three-electrode torch with a 5/16" supersonic nozzle using developed Er_2O_3/SiO_2/3% PVA powders. Detailed process parameters are presented in Tab.2.

Tab. 2 *APS and HV-APS plasma spraying parameters of the bond coat and ceramic layer*

Process parameters	Value
NiCoCrAlY bond coat (Amdry 386)	
Plasma torch type	Single-electrode torch - A60
Total flow rate of the mixture of Ar and H_2 [NLPM*]	74
Argon flow rate [NLPM]	70
Hydrogen flow rate [NLPM]	4
Power current I [A]	550
Powder flow rate [g/min]	20
Spray time [s]	340
Ceramic layer (SiO_2+Er_2O_3)	
Plasma torch type	Axial III three-electrode torch with 5/16" supersonic nozzle
Flow rate of the mixture of argon, hydrogen and nitrogen, [NLPM]	260
Argon flow rate [NLPM]	130
Hydrogen flow rate [NLPM]	30
Nitrogen flow rate [NLPM]	100
Power current [A]	220; 200; 180; 160
Powder feed rate [g/min]	10
Spraying time [s]	350
*NLPM-Normal litres per minute	

2.4 Characteristics of the produced coatings

Microscopic examinations and measurements of the produced thicknesses were performed using a Hitachi S-3400N scanning electron microscope equipped with a Thermo Scientific UltraDry EDS detector.

XRD diffraction analysis was conducted using X-ray diffractometer ARL X'TRA Thermo Scientific Corporation (CuK α radiation Bragg–Brentano geometry value of the angle 20°–80°). For identification of the phase components ICDD-PDF4-2022 crystallographic database was used.

Phase composition tests were carried out for samples of pressed and sintered powder of a mixture of silicon and erbium oxides (without the addition of a binder) at the temperature of 1450 and 1600 C for 15 h. The study was carried out to confirm that erbium silicate can actually be obtained from a mixture of these oxides. Analysis of the phase composition of the produced ceramic layers was also carried out. The aim of this study was to check whether erbium silicate could be obtained in-situ with the given parameters of plasma spraying.

3 Results and Discussion

3.1 Technological properties of granules

The most important parameter describing the technological properties of powders is the flow coefficient (dimensionless value), which is the resultant of all tested properties. Its value determines whether a given powder can fall off on its own or requires the use of additional factors, such as a vibrating table. For powders whose flow coefficient is above 80 (on a scale of up to 100), the powder does not require additional factors to facilitate its transport. Most of the obtained granulates had a value below 80. Only for the Er_2O_3+SiO_2+PVA 3% agglomerate, a result above 80 was achieved (Tab. 3). A simple experiment using a Hall funnel showed that the powder flowed without problems. For other mixtures/granulates, wedging of the powder was observed, which caused the powder to stop flowing in the funnel, which prevents its use in powder feeders used in thermal spray devices.

Tab. 3 *Technological properties of the tested powders*

Powder composition	Angle of friction internal [°]	Compressibility [%]	Angle of the flat surface [°]	Homogeneity [a.u.]	Flow coefficient [a.u.]
Er2O3+SiO_2	45.53	25.39	61.23	17.04	59.5
Er_2O_3+SiO_2+ PVA 3%	30.54	10.50	32.28	8.00	87
Er_2O_3+SiO_2+ PVA 5%	41.91	21.93	49.32	14.23	66
Er_2O_3+SiO_2+ starch 3%	44.33	22.72	56.67	15.85	62
Er_2O_3+SiO_2+ starch 5%	41.44	21.04	48.54	13.5	67
Er_2O_3+SiO_2+ cellulose gum 3%	47.52	27.46	64.98	18.75	48
Er_2O_3+SiO_2 + cellulose gum 5%	46.59	26.24	63.09	17.9	50

For all oxide powders and granules, an analysis of the grain size of the powders was performed (Tab. 4). The most reliable value is the median particle size. The obtained values are close to each other, which confirm that the method of producing powder/agglomerate mixtures is carried out correctly. No influence of the binder on the size of the agglomerate particles was observed. It can be observed that the SiO_2 powder used to prepare the mixtures is agglomerate. This can be inferred from the lack of a median particle size oscillating around the median value for SiO_2. This is probably due to the fact that during the preparation of the mixture, some of the silicon oxide particles disintegrated, which did not happen for erbium oxide, and hence the median is close to the median value for this oxide (~6.7 μm to 17.6 μm).

Tab. 4 *Powder grain size of source powders*

Powder composition	Average grain size Dn [μm]	Median grain size Dmed [μm]	Grain size fashion Dmod [μm]
Er_2O_3	7.6	6.7	5.9
SiO_2	22.9	17.6	5.9
Er_2O_3+SiO_2	8.8	6.6	5.3
Er_2O_3+SiO_2+ PVA 3%	9.5	6.5	4.8
Er_2O_3+SiO_2+ PVA 5%	8.5	6.2	4.8
Er_2O_3+SiO_2 + starch 3%	9.9	6.7	4.8
Er_2O_3+SiO_2+ starch 5%	10.0	7.4	5.3
Er_2O_3+SiO_2+ cellulose gum 3%	8.7	6.4	4.8
Er_2O_3+SiO + cellulose gum 5%	9.3	6.8	5.3

3.2 Powder morphology

Microscopic examination of the powders did not reveal differences in their morphology depending on the type and amount of organic additive present in them. Polyhedral, large silicon oxide grains and polyhedral were observed in the images or dendritic, much smaller erbium oxide grains. Due to the shape of the grains, they have a large surface area. This causes a significant friction force between the grains, which results in a decrease in the flowability of the powder.

Figure 1 shows the morphology of the powder agglomerate. Large grains of silicon oxide and grains of erbium oxide glued to them were observed (Fig. 1a). In the background visible grains of both oxides (white - erbium oxide, gray - silicon oxide). Based on the microscopic analysis, the average size of powder agglomerates was determined – 150 μm (Fig. 1b).

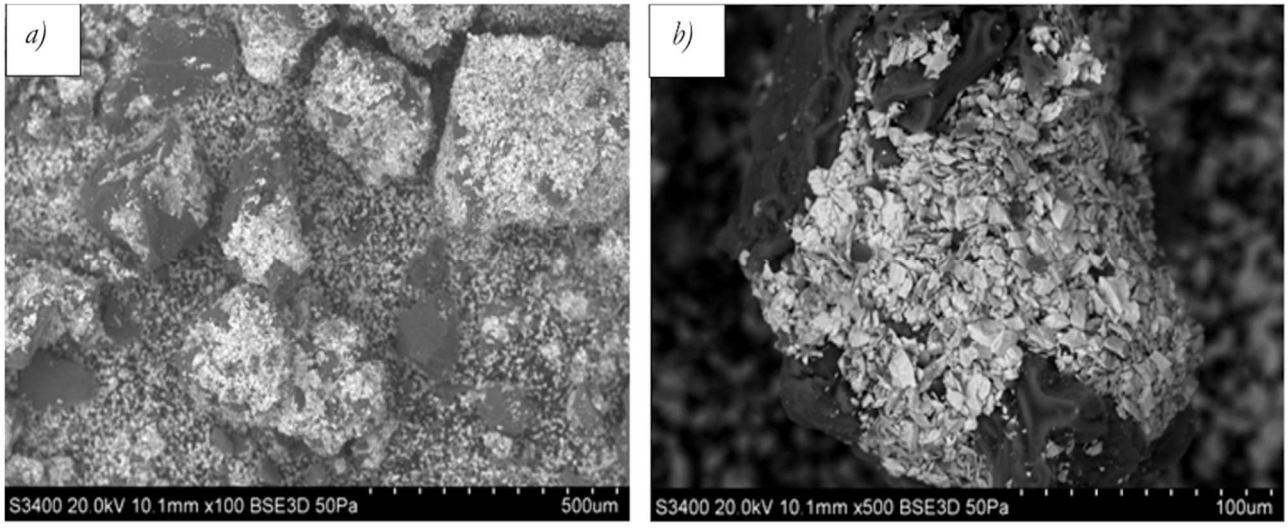

Fig. 1 *Morphology of Er_2O_3 + SiO_2 + 3% PVA powder agglomerate*

3.3 Phase composition of the reference sinter

Analysis of the phase composition of the reference material sintered at 1450 and 1600°C showed the presence of Er_2O_3 and SiO_2. (Fig. 2a, b) The results showed that sinter was heated too short. The longer time is required for the formation of Erbium silicates from manufactured powders.

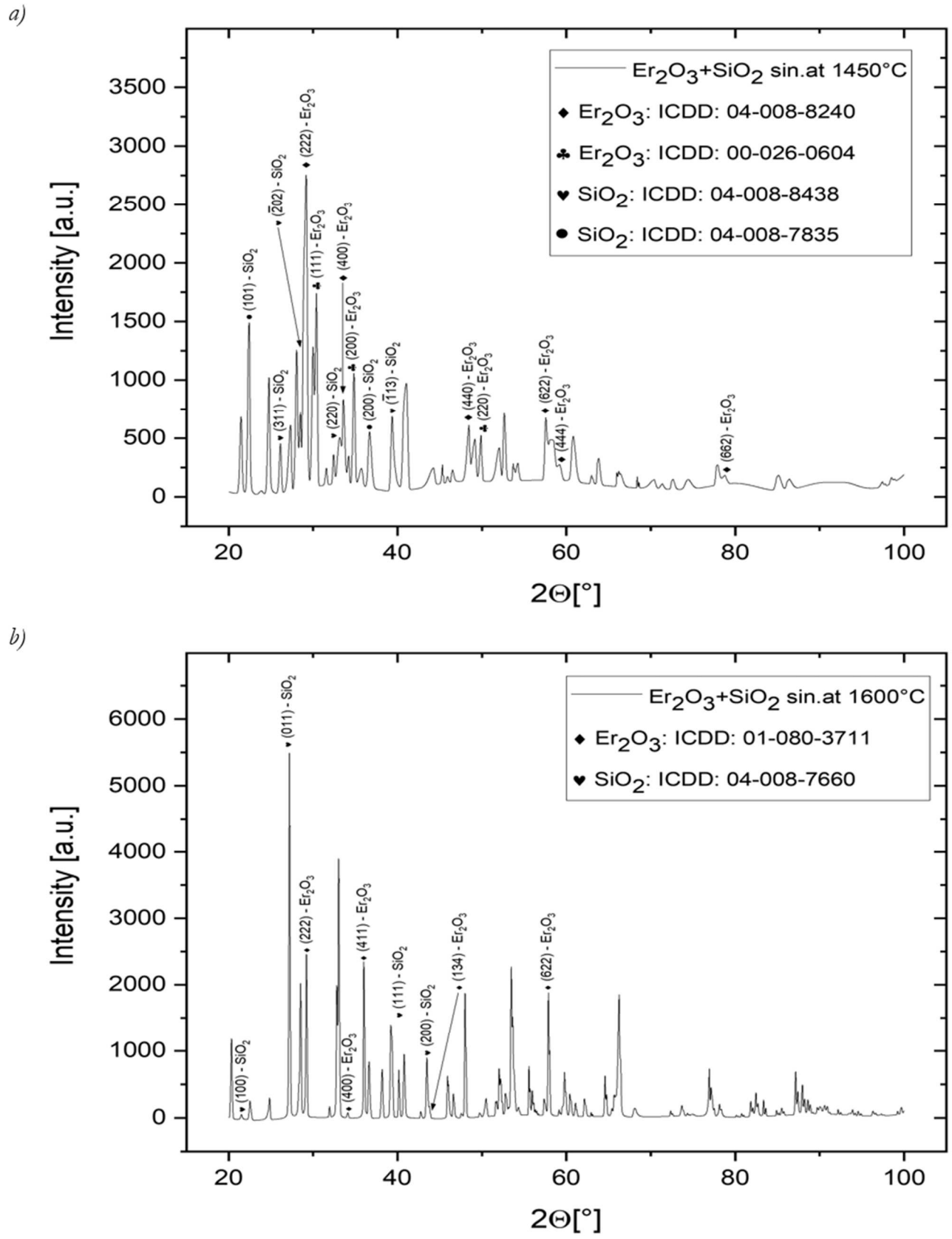

Fig. 2 *Diffractograms of reference powders sintered at 1450 °C (a) and 1600°C (b)*

3.4 Microstructure and chemical composition of obtained coating

The obtained coatings were characterized by average layer thickness 126 μm ± 10 μm. Fig. 3 shows the microstructure of the layer produced from the Er_2O_3+SiO_2 oxide mixture. The predominant white area in the ceramic layer is the matrix consisting of Er_2O_3. The grey areas are where SiO_2 occurs. Fig. 3 shows an enlargement of the selected area for better analysis of the grey areas.

To fully characterize the grey areas and confirm whether we are dealing with porosity or an area consisting of SiO_2, observations were made using optical microscopy in the bright field (Fig.4a) and in the dark field (Fig.4b). Observations in the dark field allow us to conclude that the areas visible in the bright field (and the same in the SEM method) as darker areas are areas that are not pores. The nicks visible in the enlarged area in Fig. 3 are not pores, but SiO_2 nicks created during sample preparation. To summarize the observations of the microstructure, the produced layer is a compact layer containing only micropores that are difficult to analyse and calculate.

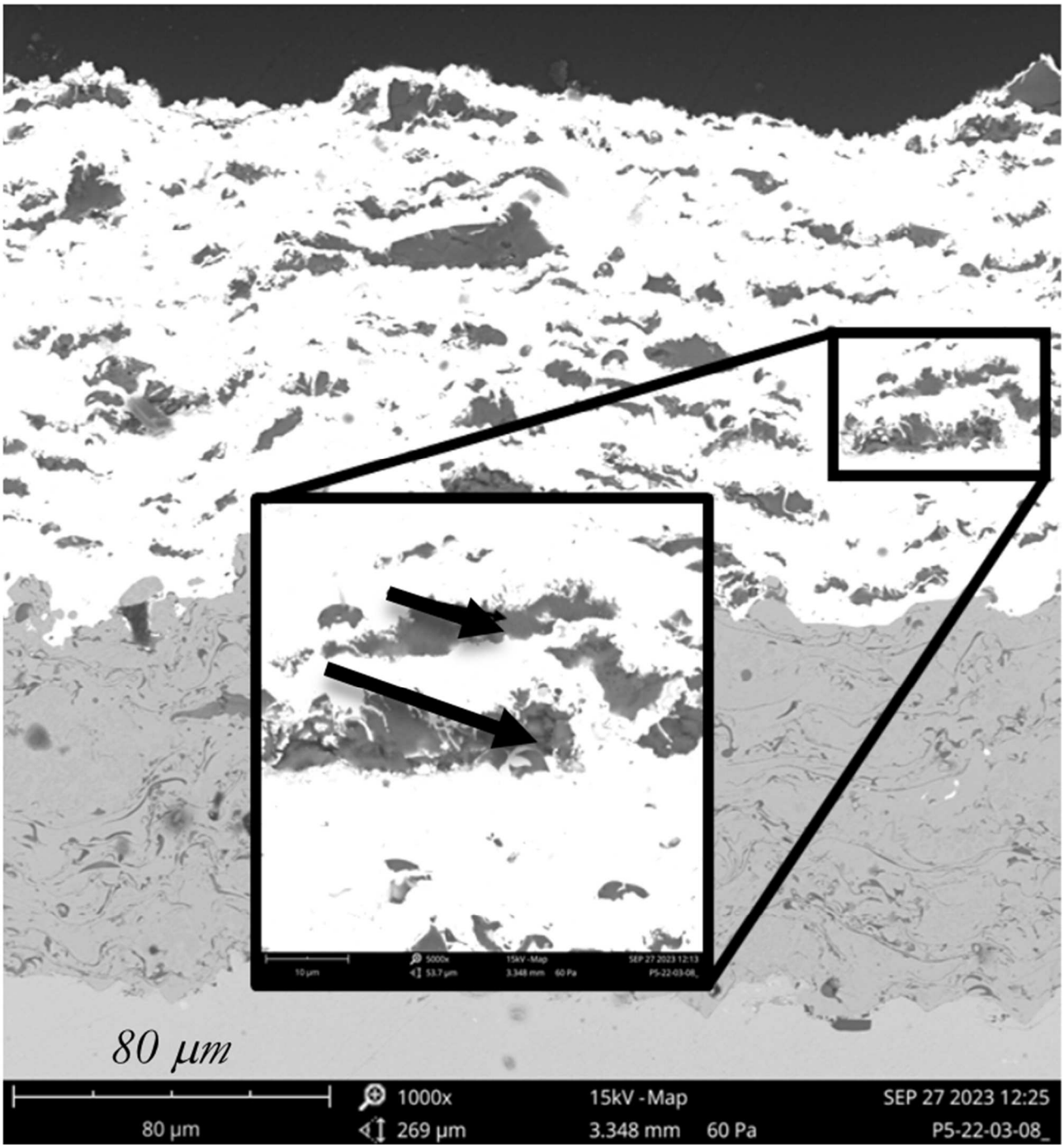

Fig. 3 *Microstructure of the produced layer observed using SEM with marked areas of potential pore occurrence*

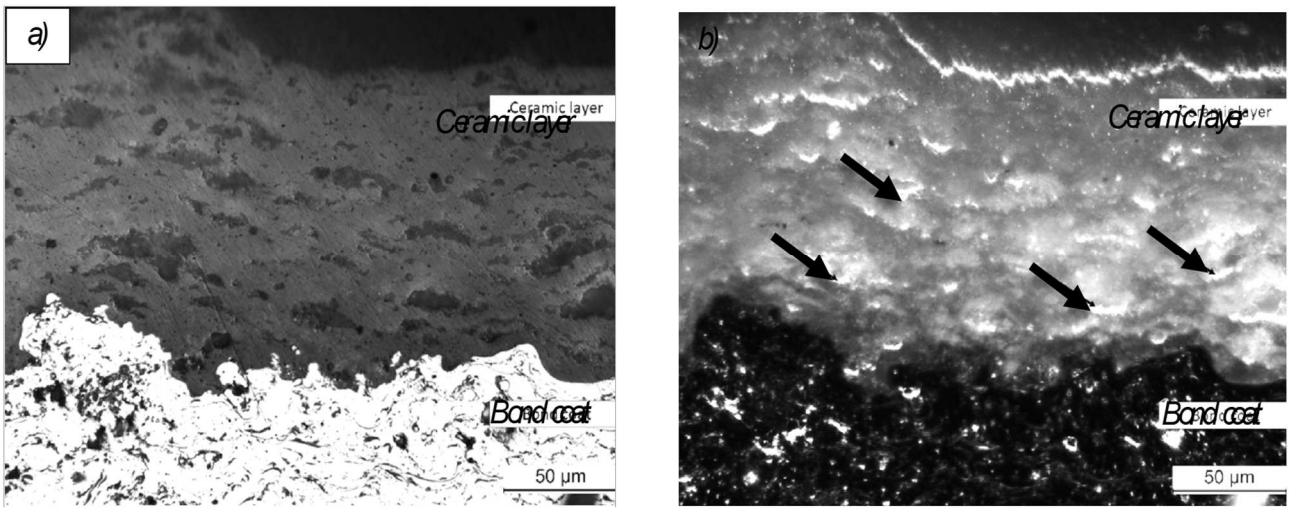

Fig. 4 *Microstructure of the produced layer observed in a) bright field, b) dark field with marks of pores*

This structure of ceramic layer was confirmed by elemental mapping (Fig. 5). Based on the analysis of microstructure photos, it was found that the distribution of elements is uniform over the entire cross-section of the coating, regardless of the process parameters used. Due to the fact that the binders added to the oxide mixtures burn easily in the plasma plume during APS process and their low content in the mixture, it can be safely assumed that the binders added to the oxide mixture were not incorporated into the produced ceramic layers.

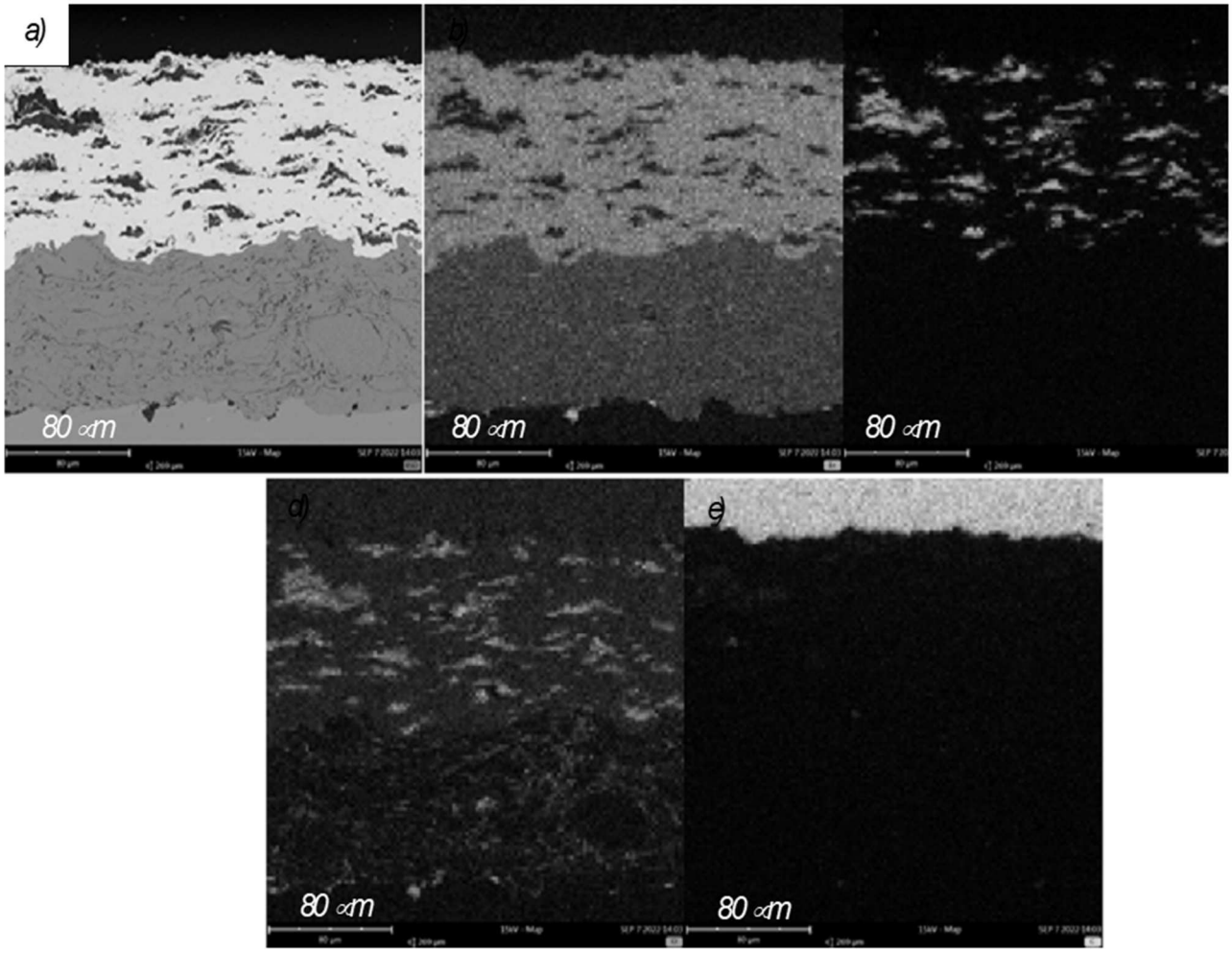

Fig. 5 *Elemental mapping of the cross-section of obtained coating after the APS plasma spraying process, using I = 220 A power current: a) BSE photo, content: b) erbium, c) silicon, d) oxygen, e) carbon*

3.5 Phase composition of the produced coatings

Analysis of the phase composition of the produced coatings showed the presence of only Er_2O_3 and SiO_2 oxides, regardless of the parameters of the APS plasma spraying process. The difractograms obtained for the coatings produced at the current intensity I = 160/180/200/220 A per electrode were presented on Fig. 6. The presence of basic powder materials – erbium and silicon oxide was only detected. This indicates that regardless of the torch current intensity and therefore the energy of the plasma plume it is not possible to synthesize erbium silicates from prepared mixtures.

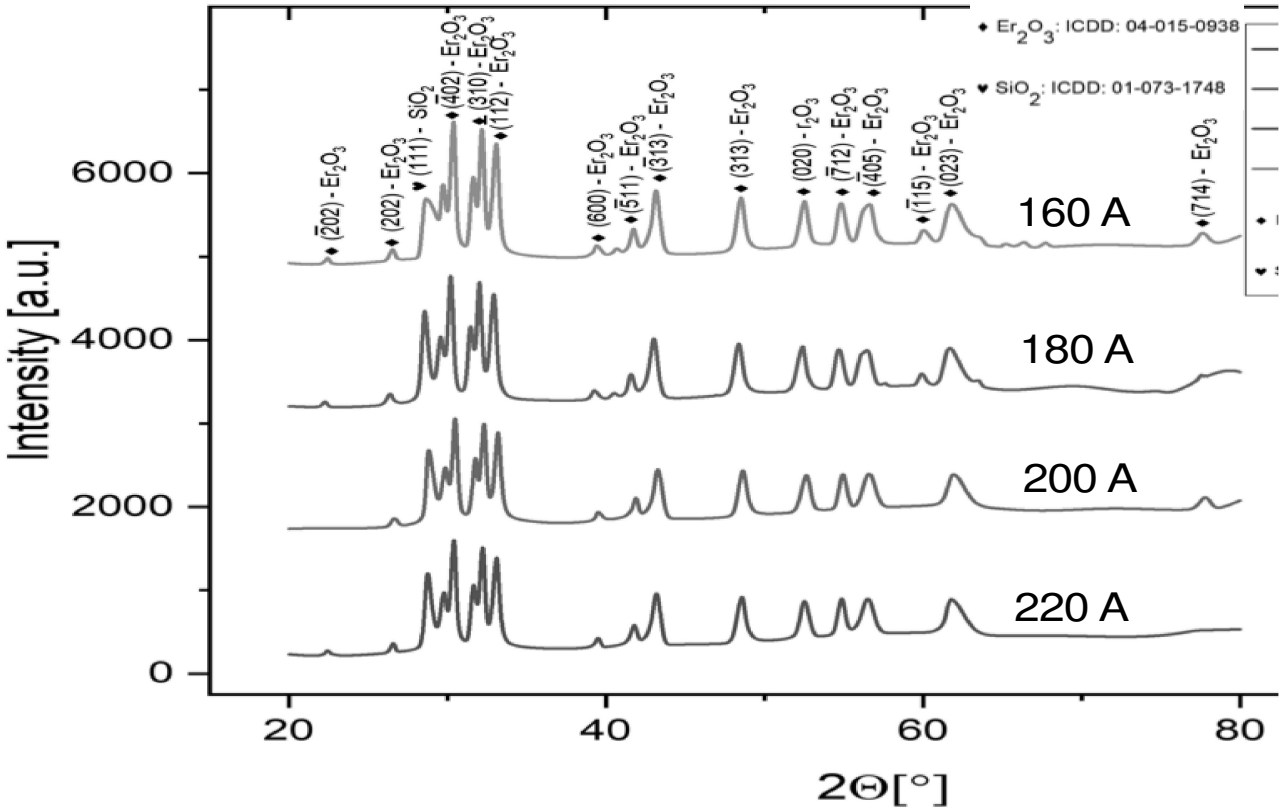

Fig. 6 *Diffractograms of the produced layers using different power current (I=160, 180, 200, 220A)*

4 Conclusions

The plasma spraying of mixture of erbium and silicon oxide was investigated. It was planned to obtain erbium silicates synthetized in plasma plume similar to formed in Reactive PS-PVD process [22,25]. The silicates, especially Ytterbium are promising materials for Environmental Barrier Coatings [13].

Organic additives such as PVA and starch in volumes of 3% and 5% improve flowability, while cellulose gum worsens it. Despite the improved flowability, it is still too small to allow free flow of powder with grain sizes of 8-10 μm in the APS Plasma Spray Tray. The dendritic and polyhedral shape of the grains and their small size cause high friction forces between the powder particles, which prevents the transfer of the powder from the feeder to the plasma torch. Making powder agglomerates with an average size of 150 μm with the addition of 3% PVA leads to a significant decrease in the surface area of powder grains. This results in a significant increase in flowability and allows it to be used as a charge material for APS plasma spraying.

The powder agglomerate makes it possible to create a layer consisting of erbium oxide and silicon oxide, evenly distributed over the cross-section of the layer. However, it is not possible to synthesize erbium silicate directly in the APS process due to the too low temperature of the plasma flame and the too low energy of the flame itself. The material was only melted, not vaporized. Changing the current intensity during the APS thermal spraying process does not affect the morphology of the produced coating, phase composition and the distribution of elements on its cross-section. The energy of the plasma spraying process using the APS method is too low for synthesis of erbium disilicate in the resulting coating. However,it is not possible to synthesize erbium silicate directly in the APS process due to the too low temperature of the plasma flame and the too low energy of the flame itself. The material was only melted, not vaporized. Changing the power current during the APS thermal spraying process does not affect the morphology of the produced coating, phase composition and the distribution of elements on its cross-section.

On the other hand, Re_2O_3 oxide mixtures have been analysed for many years as materials for TBC coatings [28]. The erbium oxide might be used in this application [29] and as mixture with other ReO oxides. Developed coatings and HV-APS methods could be used as a bond coat/interlayer for other composition of EBCs for Ceramic Matrix Composites [30].

References

[1] BELAN J, VAŠKO A, KUCHARIKOVÁ L, TILLOVÁ E, CHALUPOVÁ M. (2019), The SEM Metallography Analysis of Vacuum Cast ZhS6K Superalloy Turbine Blade after Various Working Hours. In: *Manufacturing Technology*.;19(5):727-733. doi: 10.21062/ujep/362.2019/a/1213-2489/MT/19/5/727.

[2] MA, L.J., H. YU, X.H. MAO, C.R. LI, C.Y. FENG, F.N. LI. (2023). Influence of Cutting Tool and Drilling Process on the Machinability of Inconel 718. In: *Manufacturing Technology*, 23(2): 204-215, DOI: 10.21062/mft.2023.013

[3] JOPEK, J., MOKRZYCKA, M., GÓRAL, M., KOSCIELNIAK, B., OCHAL, K., DRAJEWICZ, M. (2023), High Temperature Protective Coatings for Aeroengine Applications. In: *Manufacturing Technology*, 23 (4), 436-448., DOI: 10.21062/mft.2023.052

[4] CHOWDHURY, T.S., MOHSIN, F.T., TONNI, M.M., MITA, M.N.H., EHSAN, M.M., (2023), A critical review on gas turbine cooling performance and failure analysis of turbine blades, In: *International Journal of Thermofluids*, 18, 100329, https://doi.org/10.1016/j.ijft.2023.100329

[5] KRBATA, M.; FABO, P.; KOHUTIAR, M.; ESCHEROVA, J.; KUBA, M.; KIANICOVA, M.; ECKERT, M., (2023), Possibilities of Using Impedance Spectroscopy for Indirect Measurements of Thin Layers of Al & Cr-Al Coatings on Ni-based Superalloy Inconel 713LC Applied by the "Out-of-pack" Diffusion Method. In: *Manufacturing Technology* 23 (3), 313-318, DOI: 10.21062/mft.2023.042

[6] BARWINSKA, I., KOPEC, M., KUKLA, D., SENDEROWSKI, C., KOWALEWSKI, Z.L., (2023), Thermal Barrier Coatings for High-Temperature Performance of Nickel-Based Superalloys: A Synthetic Review, In: *Coatings*, 13 (4), 769, DOI: 10.3390/coatings13040769

[7] GORAL, M., PYTEL, M., SOSNOWY, P., KOTOWSKI, S., DRAJEWICZ, M., (2013), Microstructural characterization of thermal barrier coatings deposited by APS and LPPS thin film methods, In: *Solid State Phenomena*, 197, 1–5, https://doi.org/10.4028/www.scientific.net/SSP.197.1

[8] PĘDRAK, P., DRAJEWICZ, M., DYCHTOŃ, K., NOWOTNIK, A., (2016), Microstructure and thermal characteristics of $SiC–Al_2O_3–Ni$ composite for high-temperature application, In: *Journal of Thermal Analysis and Calorimetry*, 125 (3), 1353–1356, https://doi.org/10.1007/s10973-016-5608-2

[9] MOREL, C., BARANGER, E., LAMON, J., BRAUN, J., LORRETTE, C., (2023), The influence of internal defects on the mechanical behavior of filament wound SiC/SiC composite tubes under uniaxial tension, In: *Journal of the European Ceramic Society*, 435, 1797-1807, DOI10.1016/j.jeurceramsoc.2022.12.040

[10] LÜ, X., LI, L., SUN, J., YANG, J., JIAO, J., (2023), Microstructure and tensile behavior of (BN/SiC)n coated SiC fibers and SiC/SiC minicomposites, In: *Journal of the European Ceramic Society*, 435, 1828-1842, DOI10.1016/j.jeurceramsoc.2022.12.032

[11] ZOK, F.W., MAXWELL, P.T., KAWANISHI, K., CALLAWAY, E.B., (2020), Degradation of a SiC-SiC composite in water vapor environments, In: *Journal of the American Ceramic Society*, 1033, 1927-1941, https://doi.org/10.1111/jace.16838

[12] FAUCETT, D.C., CHOI, S.R., (2011), In: *Proceedings of the ASME Turbo Expo 1*, 497-504, DOI 10.1115/GT2011-46771

[13] MOKRZYCKA M., JOPEK J., SŁYŚ. A, GÓRAL M., OCHAŁ K., (2023), Modern materials used for environmental barrier coatings – a review, *Ochrona Przed Korozją*, 4, 104-112, DOI:10.15199/40.2023.4.2

[14] LEE, K. N. (2015). Environmental Barrier Coatings for SiC/SiC. In: *John Wiley and Sons*

[15] TEJERO-MARTIN, D.; BENNETT, C.; HUSSAIN, T. (2021) A review on environmental barrier coatings: History, current state of the art and future developments. In: *Journal of the European Ceramic Society*, 41, 1747-1768, https://doi.org/10.48550/arXiv.2007.14914

[16] XU, J., SARIN, V., BASU, S., (2012), Stability study of EBC/TBC hybrid system on Si-based ceramics in gas turbines, In: *Materials Research Society Symposium Proceedings*, 1519, 21-27, DOI 10.1557/opl.2012.1717

[17] RICHARDS, B. T.; WADLEY, H.N.G. (2014) Plasma spray deposition of tri-layer environmental barrier coatings. In: *Journal of the European Ceramic Society*, 34, 3069-3083, https://doi.org/10.1557/opl.2012.1717

[18] GRACIA, E.; LEE, H.; SAMPATH, S. (2019) Phase and microstructure evolution in plasma sprayed Yb2Si2O7 coatings. *Journal of the European Ceramic Society*, 39, 1477-1486, https://doi.org/10.1016/j.jeurceramsoc.2018.11.018

[19] RICHARDS, B. T.; SEHR, S.; DE FRANQUEVILLE, F.; BEGLEY, M. R.; WADLEY, H.N.G. (2016) Fracture mechanisms of ytterbium monosilicate environmental barrier coatings during cyclic thermal exposure. In: *Acta Materialia*, 103, 448-460, https://doi.org/10.1016/j.actamat.2015.10.019

[20] RICHARDS, B. T.; BEGLEY, M. R.; WADLEY, H. N. G. (2015) Mechanisms of Ytterbium Monosilicate/Mullite/Silicon Coating Failure During Thermal Cycling in Water Vapor. In: *Journal of the American Ceramic Society*, 98 (2), 4066-4075, DOI: 10.1111/jace.13792

[21] TURCER, L.R., KRAUSE, A.R., GARCES, H.F., ZHANG, L., PADTURE, N.P., (2018), Environmental-barrier coating ceramics for resistance against attack by molten calcia-magnesia-aluminosilicate (CMAS) glass: Part II, β-$Yb_2Si_2O_7$ and β-$Sc_2Si_2O_7$, In: *Journal of the European Ceramic Society*, 3811, 3914-3924, DOI 10.1016/j.jeurceramsoc.2018.03.010

[22] PĘDRAK, P., DYCHTOŃ, K., DRAJEWICZ, M., GÓRAL, M., (2021), Synthesis of gd2zr2o7 coatings using the novel reactive ps-pvd process, In: *Coatings*, 1110, 1208, DOI 10.3390/coatings11101208

[23] ROKICKI, P., GÓRAL, M., KUBASZEK, T., DYCHTON K., DRAJEWICZ M., WIERZBIŃSKA, M., OCHAL, K., (2022), The microstructure and thermal properties of Yb_2SiO_5 coating deposited using APS and PS-PVD methods, *Archives of Materials Science and Engineering*, 114, (2), 49–57, DOI10.5604/01.3001.0016.0025

[24] KUBASZEK, T., NOWAK, W., PĘDRAK, P., TRYBUS, K., ŚLEMP, K. GÓRAL, M. (2019) "The formation of pyrochlores during plasma spraying of REO and zirconia oxides powder mixture", In: *Journal of Mechanical and Energy Engineering*, 3 (2), 141-148. doi: 10.30464/jmee.2019.3.2.141.

[25] PĘDRAK, P., GÓRAL, M., DYCHTON, K., WIERZBINSKA, M., KUBASZEK, T., (2022), The Influence of Reactive PS-PVD Process Parameters on the Microstructure and Thermal Properties of Yb_2 Zr_2O_7 Thermal Barrier Coating, In: *Materials*, 154, 1594, DOI 10.3390/ma15041594

[26] KUBASZEK, T., GÓRAL, M., SŁYŚ, A., SZCZĘCH D., GANCARCZYK, K., DRAJEWICZ, M., The influence of HV-APS process parameters on microstructure and erosion resistance of metalloceramic WC-CrC-Ni coatings, In: *Ceramics International*, 49 (1),18007–18013, https://doi.org/10.1016/j.ceramint.2023.02.148

[27] NOWAK W., KUBASZEK T., GÓRAL M., WIERZBA B., (2020), Durability of underaluminized thermal barrier coatings during exposure at high temperature, In: *Surface and Coatings Technology,* 382, 125236, https://doi.org/10.1016/j.surfcoat.2019.125236

[28] DUDNIK, O.V., LAKIZA, S.M., GRECHANYUK, I.M., REDKO V.P., MAKUDERA A.A., GLABAY M.S., MAREK I.O, RUBAN, A.K., GRECHANYUK, M.I. (2021), Composite Ceramics for Thermal Barrier Coatings Produced From ZrO_2 Doped with Yttrium-Subgroup Rare-Earth Metal Oxides, In: *Powder Metallurgy and Metal Ceramics,* 5911-12, 672–680, https://doi.org/10.1007/s11106-021-00202-8

[29] WANG, Q., GUO, L., YAN, Z., YE, F., (2018), Phase composition, thermal conductivity, and toughness of TiO2-doped, Er_2O_3-stabilized ZrO_2 for thermal barrier coating applications, In: *Coatings*, 8 (7), 253, https://doi.org/10.3390/coatings8070253

[30] MIRANDA, F.S., CALIARI, F.R., CAMPOS, T.M., Leite, D.M.G., PESSOA R., ESSIPTCHOUK, A.M., PETRACONI, G., (2020) High-velocity plasma spray process using hybrid SiO_2 + ZrO_2 precursor for deposition of environmental barrier coatings, In: *Surface and Coatings Technology*, 404, art. no. 126447, https://doi.org/10.1016/j.surfcoat.2020.126447